Mycobacterial pan-genome analysis suggests important role of plasmids in the radiation of type VII secretion systems

Emilie Dumas, Eva Christina Boritsch, Mathias Vandenbogaert, Ricardo C. Rodriguez de La Vega, Jean-Michel Thiberge, Valerie Caro, Jean-Louis Gaillard, Beate Heym, Fabienne Girard-Misguich, Roland Brosch, et al.

To cite this version:

Emilie Dumas, Eva Christina Boritsch, Mathias Vandenbogaert, Ricardo C. Rodriguez de La Vega, Jean-Michel Thiberge, et al.. Mycobacterial pan-genome analysis suggests important role of plasmids in the radiation of type VII secretion systems. Genome Biology and Evolution, Society for Molecular Biology and Evolution, 2016, 8 (2), pp.387-402. <10.1093/gbe/evw001>. <hal-01291528>

HAL Id: hal-01291528
http://hal.upmc.fr/hal-01291528

Submitted on 21 Mar 2016

Genome Biology and Evolution Advance Access published January 8, 2016 doi:10.1093/gbe/evw001

Mycobacterial pan-genome analysis suggests important role of plasmids in the radiation of type VII secretion systems

Emilie Dumas[1], Eva Christina Boritsch[2], Mathias Vandenbogaert[3], Ricardo C Rodrı́guez de la Vega[4], Jean-Michel Thiberge[3], Valerie Caro[3], Jean-Louis Gaillard[1,5], Beate Heym[1,5], Fabienne Girard-Misguich[1], Roland Brosch[2*], Guillaume Sapriel[1,6,7*].

[1]INSERM U1173, UFR Simone Weil, Versailles-Saint-en-Quentin University, 78180 Saint-Quentin-en-Yvelines, France;

[2] Institut Pasteur, Unit for Integrated Mycobacterial Pathogenomics, 75724 Paris Cedex 15, France;

[3] Institut Pasteur, Genotyping of Pathogens and Public Health, 75724 Paris Cedex 15, France;

[4] UMR8079, Ecologie Systématique Evolution, Univ. Paris-Sud, CNRS, Université Paris-Saclay, 91400, Orsay, France;

[5] AP-HP, Hôpital Ambroise Paré, Service de Microbiologie et Hygiène, Boulogne-Billancourt, France;

[6] UMR 8212, LSCE, Versailles-Saint-Quentin University, 78180 Saint-Quentin-en-Yvelines, France;

[7] Atelier de Bio-informatique. Institut de Systématique, Evolution, Biodiversité, ISYEB, UMR 7205, CNRS, MNHN, UPMC, EPHE. Muséum national d'Histoire naturelle, 75231 Paris Cedex 05, France.

*For correspondence:

Roland Brosch, email: roland.brosch@pasteur.fr

Guillaume Sapriel, email: guillaume.sapriel@uvsq.fr

Manuscript type: Article

Keywords: mycobacteria, tuberculosis, virulence, horizontal gene transfer, phylogeny, ESX / type VII secretion systems, mycobacterial evolution.

Abstract

In mycobacteria, various type VII secretion systems corresponding to different ESX (ESAT-6 secretory) types, are contributing to pathogenicity, iron acquisition, and/or conjugation. In addition to the known chromosomal ESX loci, the existence of plasmid-encoded ESX systems was recently reported. To investigate the potential role of ESX-encoding plasmids on mycobacterial evolution we analysed a large representative collection of mycobacterial genomes, including both chromosomal and plasmid-borne sequences. Data obtained for chromosomal ESX loci confirmed the previous 5 classical ESX types and identified a novel mycobacterial ESX-4-like type, termed ESX-4-bis. Moreover, analysis of the plasmid-encoded ESX loci showed extensive diversification, with at least 7 new ESX profiles, identified. Three of them (ESX-P clusters 1, 2 and 3) were found in multiple plasmids, while four corresponded to singletons. Our phylogenetic and gene-order-analyses revealed two main groups of ESX types: i) ancestral types, including ESX-4 and ESX-4-like systems from mycobacterial and non-mycobacterial actinobacteria, and ii) mycobacteria-specific ESX systems, including ESX-1-2-3-5 systems and the plasmid-encoded ESX types. Synteny analysis revealed that ESX-P systems are part of phylogenetic groups that derived from a common ancestor, which diversified and resulted in the different ESX types through extensive gene rearrangements. A converging body of evidence, derived from composition bias-, phylogenetic- and synteny analyses points to a scenario in which ESX-encoding plasmids have been a major driving force for acquisition and diversification of type VII systems in mycobacteria, which likely played (and possibly still play) important roles in the adaptation to new environments and hosts during evolution of mycobacterial pathogenesis.

Introduction

Mycobacteria represent a prokaryotic genus with a vast diversity of lifestyles, ranging from major human pathogens, such as *Mycobacterium tuberculosis*, opportunistic pathogens, such as *Mycobacterium abscessus*, to environmental saprophytes that represent the great majority of mycobacterial species (Magee and Ward 2012; Boritsch, *et al.* 2014). Mycobacteria are classified into rapidly growing mycobacteria (RGM), making visible colonies on solid media in less than one week of incubation, and slowly growing mycobacteria (SGM), which is a monophyletic cluster (Mignard and Flandrois 2008) that contains the major mycobacterial pathogens. Mycobacteria are characterized by an impermeable diderm cell envelope formed by a cytoplasmic membrane, a peptidoglycan and an arabinogalactan-layer, long-chain mycolic acids and extractable lipids (Kaur, *et al.* 2009; Le Chevalier, *et al.* 2014), which contributes to the natural resistance of mycobacteria to many environmental stresses, biocides and antibiotics.

Protein transport across this thick and complex mycobacterial cell envelope is carried out by different secretion systems, including the so-called ESX systems. These systems were named after the first identified substrate, the 6 kDa early secretory antigenic target (ESAT-6) (Brodin, *et al.* 2004), and more recently were also termed type VII secretion systems (Abdallah, *et al.* 2007; Majlessi, *et al*. 2015). The typical ESX-secretion apparatus is constituted of a membrane-linked complex of at least 4 ESX-conserved-components (EccB, EccC, EccD, and MycP), ESX-type-specific associated proteins (EspA, EspB, EspC, EspG, etc), and secreted/exported proteins, such as ESAT-6 and CFP-10, and/or PE and PPE proteins (Majlessi, *et al*. 2015). The variation in the genetic organization of individual ESX systems defines 5 ESX subtypes in *M. tuberculosis* that are named ESX-1 to ESX-5 (Bitter, *et al.* 2009).

The ESX-1 secretion system is a key component involved in *M. tuberculosis* pathogenicity (Majlessi, *et al*. 2015), which is non-functional in the attenuated, closely related *Mycobacterium bovis* BCG vaccine due to the partial loss of the ESX-1-encoding genomic region, named region of difference 1 (RD1) (Mahairas, *et al.* 1996; Behr, *et al.* 1999; Pym, *et al.* 2002). Protein secretion via this specialized ESX-1 system plays an important role for host–pathogen interaction of *M. tuberculosis* (Majlessi, *et al.* 2015) and other pathogenic mycobacteria (Abdallah, *et al.* 2007), enabling vacuolar rupture and cytosolic contact within host macrophages (Houben, *et al.* 2012; Simeone, *et al.* 2015). Moreover, other ESX systems are also involved in important biological functions of mycobacteria. While ESX-3 plays a role in iron and zinc uptake (Serafini, *et al.* 2009; Siegrist, *et al.* 2014) the function of ESX-5 is linked to the export of PE and PPE proteins and pathogenicity (Abdallah, *et al.* 2009; Bottai, *et al.* 2012; Sayes, *et al*. 2012).

Apart from protein secretion, ESX-1 systems are also involved in chromosomal DNA transfer through conjugation (Coros, *et al.* 2008; Gray, *et al.* 2013). In *Mycobacterium smegmatis,* the chromosomally encoded ESX-1 system enables unconventional genome-wide genetic exchanges between donor and recipient strains, named “distributive conjugal transfer” (Gray, *et al.* 2013; Mortimer and Pepperell 2014). A recent study also describes conjugation events between strains of *Mycobacterium marinum* that involve a new class of plasmids encoding elements of type VII and type IV secretion systems, and a relaxase (Ummels, *et al.* 2014).

Thus, in mycobacteria, ESX systems govern diverse important biological functions for host-pathogen interaction and inter-strain genetic transfer. Although some insights into the genetic organization and distribution of ESX systems among selected mycobacteria are available from previous studies (Cole, *et al.* 1998; Tekaia, *et al.* 1999; Gey Van Pittius, *et al.* 2001), systematic large-scale screening data for typeVII/ESX components in mycobacterial genomes are not yet available. This led us to use an extensive, pan-genome-wide approach together with a large-scale Hidden Markov Model profile-based screen, to investigate the distribution of ESX systems in the large variety of mycobacterial chromosomes and plasmids. This study allowed us to identify a wide diversity of ESX systems in mycobacteria and to identify new, plasmid-encoded ESX-systems. Moreover, the generated deep phylogeny data and results from synteny analyses of the different ESX systems suggested that plasmid-encoded ESX clusters were substantially contributing to ESX diversification as well as to plasmid-chromosome genetic exchanges of ESX-associated genes and systems. Our results thus suggest an important contribution of ESX-encoding plasmids in long-term mycobacterial evolution, and more specifically in the evolution of ESX-mediated *M. tuberculosis* pathogenicity determinants, such as ESX-1 and/or ESX-5.

Materials and Methods

Mycobacterial genome and plasmids database

The *National Center for Biotechnology Information* (NCBI) public database was used to build a representative set of mycobacterial sequences. When several sequences were available for a given species, the genome with the highest level of completeness was chosen based on the NCBI Genome Assembly and Annotation report (Supplementary table S1). All available mycobacterial plasmids that were fully assembled at the time of the database interrogation (July 2014) were introduced into the database (Supplementary table S2).

Strains from this study

In addition to the sequences retrieved from the NCBI database, we added the sequences from two additional strains. One of them was taken from a clinical collection of *M. abscessus* isolates, and this strain was called *M. abscessus subsp. bolletii* strain 5625. The other strain was an environmental isolate from the Paris tap water network, belonging to the phylogenetic group of RGM *M. aubagnense*, and was called *M. sp. 960*. *M. abscessus subsp. bolletii* strain 5625 was introduced into the study because initial analysis of the assembled genome contig-sequences suggested that this strain contained a plasmid encoding ESX elements. Strain *M. sp. 960* was added, because no other genome information on the *M. aubagnense* phylogenetic group was yet published/available. NGS-derived sequence (SRA) reads from *M. sp. 960* and *M. abscessus subsp. bolletii* strain 5625 were submitted to NCBI, and their accession numbers are respectively SRR1951096 and SRR1951800.

Genome sequencing and assembly

Paired-end Illumina libraries were constructed from 50 nanogram of genomic DNA according to the Epicentre Nextera protocol. A set of Nextera-compatible adaptor primers containing index sequences was used. Template amplification was performed using a cBot automated cluster generation system. Sequencing was performed on an Illumina HiSeq 2000 instrument (Illumina), using a read length of 50 or 100 bp. All library pools were treated as paired-end sequences. To ensure high data quality for various downstream analyses, such as sequence assembly, raw reads were subjected to a number of pre-processing ‘‘cleaning’’ steps: (1) reads bearing a number of bases with sufficiently high Phred quality score were selected (using Sanger quality > 20 and remaining read length > 30 nt as thresholds); (2) primer/adaptor sequence were excised from the remaining reads; (3) reads with lengths less than a given threshold were removed; (4) homopolymer-containing reads were trimmed and (5) duplicated reads were identified and removed. Remaining reads were *de novo* assembled with CLC Genomics Workbench version 3 (CLC Bio, Cambridge, MA). Resulting sequence contigs were checked by comparison to the *M. abscessus* ATCC 19977 (Genbank ACC NC_010397) reference sequence, using the MUMmer package (Delcher, *et al.* 2002).

ESX-loci annotation

Prokaryotic GeneMark.hmm (version 2.8) (Besemer and Borodovsky 2005), was used to predict ORFs on mycobacterial genomes and plasmids available in the GenBank database or sequenced in this study (Supplementary tables S1 and S2). Similarity searches were performed based on protein domains using HMMer package (Finn, *et al.* 2011) (version 3.1b1), with ESX motifs previously identified in mycobacterial genomes: EccA (TIGR03922), EccB (TIGR03919), EccC (TIGR03924 and TIGR03925), EccD (TIGR03920), EccE (TIGR03923), MycP (TIGR03921), Esx (ESAT-6/CFP10 proteins: TIGR03930) and PPE (PF00823). PE, and EspG proteins were identified by similarity searches using BLASTP (Altschul, *et al.* 1990) against mycobacterial genome sequences. An e-value threshold filter was introduced for each protein family in order to minimize the number of wrongly identified ESX encoding genes. For each gene, the e-value threshold was determined based on the e-value distribution.

Phylogeny

Sequence alignments and curating was performed using MUSCLE and Gblocks, implemented in the Phylogeny.fr website (Dereeper, *et al.* 2008). MEGA software (Tamura, *et al.* 2013) was used for phylogenetic tree construction using a maximum likelihood method with 250 bootstrap replicates and for generating best-fit models of evolution. Graphical representations of phylogenetic trees of individual genes were performed using iTOL (Letunic and Bork 2011). Phylogenetic trees at the gene level were obtained for EccB, EccC, MycP, followed by alignment of concatenated sequences of EccB, EccC and MycP proteins, which was used to reconstruct the phylogeny of the ESX loci.

Comparative genomics

Comparative genomics studies were performed on the Microbial Genome Annotation & Analysis Platform MaGe (Magnifying Genomes) (Vallenet, *et al.* 2009), including synteny analysis, mobile elements identification, and genomic island detection. Composition bias detection was performed using Alien hunter software (Vernikos and Parkhill 2006). Plasmid and contig alignments at the nucleotide level were performed using Artemis Comparison Tool (Carver, *et al.* 2005).

To estimate the level of gene conservation, pairwise dN/dS ratio ω (dN: non-synonymous mutation substitution rate, dS: synonymous mutation substitution rate) were calculated using the program CODEML provided by the PAML (Phylogenetic Analyses by Maximum Likelihood) package version 4 (Yang 1997). Nucleotidique sequences have been aligned using TranslatorX (Abascal, *et al.* 2010) guided by protein sequence alignments obtained using M-coffee (Wallace, *et al.* 2006).

Recombination analysis was achieved using RDP4 version Beta 4.46 (Martin, *et al.* 2015). Six methods including RDP, GENECONV, Bootscan, Maxchi, Chimaera and SiScan implemented in RDP4 were used to detect recombination events, likely parental isolates and recombination break points under default settings.

Tree topology tests

As no *a priori* hypothesis for the phylogenetic placement of plasmid-borne ESX systems exists, we generated 85 bootstrapped trees of the concatenated alignment with PhyML (Guindon, *et al.* 2010) under the LG+G+I+F amino acid substitution model (the best fit model according to ProtTest (Abascal, *et al.* 2005). Site-wise log-likelihood values of the 85 bootstrapped trees and the best tree obtained with MEGA were obtained with TreePuzzle (Schmidt, *et al.* 2002) and fed into Consel (Shimodaira and Hasegawa 2001) to perform the approximately unbiased (AU) test of tree topologies. Monophyly of three plasmid-borne ESX clusters, the five ESX chromosomal types, and the sister relationships: ESX-P cluster 1 – ESX-5; ESX-P cluster 2 – (ESX-P cluster 3 – ESX-2); ESX-P cluster 4 – ESX-3 and ESX-4-bis – ESX-4 were assessed using Consel.

PFGE and Southern Blot hybridization

Agarose plugs containing total genomic DNA from *M. abscessus subsp. bolletii* strain 5625 were prepared as previously described (Brosch, *et al.* 2000). Non-digested DNA preparations were separated on a 1% (w/v) agarose gel by pulsed-field gel electrophoresis (PFGE) on a Biorad CHEF II apparatus with a pulse of 5 s ramping to 35 s for 23 h at 6 V/cm. Low-range PFG marker (NEB) was used as a size standard, and total genomic DNA from *Mycobacterium canettii*, known to lack plasmids (Supply, *et al.* 2013), as negative control. Under such PFGE migration conditions, large plasmids migrate inside the gelmatrix, while intact chromosomal DNA is unable to migrate (Stinear, *et al.* 2004). DNA was transferred onto a Hybond-C Extra nitrocellulose membrane (Amersham) as described in (Brosch, *et al.* 2000) with some modifications. PCR-derived DNA probes were labelled with [α^{32}P] dCTP using the Prime-It II kit (Stratagene), followed by hybridization at 68°C in 6x SSC/ 0.5% SDS/ 0.01 M EDTA/ 5 x Denhardt's solution/ 100 μg/ml single-stranded salmon sperm DNA. The membrane was washed first for 5 min at room temperature in 2x SSC/ 0.5% SDS, then for 15 min in 2x SSC/ 0.1% SDS and finally for 1 h in 1x SSC/ 0.5% SDS. The membrane was exposed on a phosphorimager screen and revealed using a STORM phosphorimager. The probes were amplified by PCR from *M. bolletti* pMBOL DNA with specific primers 5625-F (5'-AGGTACCAGCTCAAGGGAAC) and 5625-R (5'-GCATGGTGTTGGTGACGTTT), designed on *M. bolletti* pMBOL ESX-plasmid using Primer3 software (Koressaar and Remm 2007). PCR reaction conditions were as following: 100 ng of genomic DNA were added to the reaction mixture containing 2 μM of each primer, 0.5 units of Taq polymerase (ampliTaq, Applied Biosystems), PCR buffer (10% DMSO, 0.5 mM dNTP, 60 mM TrisHCl, pH 8.8, 2 mM $MgCl_2$, 17 mM $(NH_4)_2SO_4$, 10 mM β-mercaptoethanol) and sterile distilled water to 25 μl. PCR amplification conditions were as follows: initial denaturation of 94 ° C for 5 min, 30 cycles of 94° C for 30 s, 54° C for 60 s, 72° C for 45 s followed by a final extension of 72° C for 10 min (Biorad). A PCR clean-up was performed (Macherey Nagel) and the purified fragments were double strand sequenced to confirm probes. To determine the contiguity and order of the two non-aligned contigs that contained ESX sequences in the *M. abscessus subsp. bolletii* 5625 strain, PCR primers were designed at the 5' and 3' ends of each contig covering all different contiguity possibilities. PCR products were then verified by sequencing, allowing to determine gene order and to confirm that each of these two non-aligned contigs contained a part of a single new ESX locus that was then probe-targeted for PFGE assay as described above.

Results

Identification of new ESX loci in mycobacterial plasmids

In order to identify ESX-containing chromosomal loci and plasmids, we used the HMMER software (Finn, *et al.* 2011) to launch motif searches corresponding to TIGR03922 (EccA), TIGR03919 (EccB), TIGR03924 (EccC), TIGR03920 (EccD) and TIGR3921 (MycP), in mycobacterial sequences from the NCBI database and in contig sequences from our clinical collection of *M. abscessus* isolates. In total, we identified at least one or more full ESX locus/loci in 41 mycobacterial (22 RGM and 19 SGM strains) and in the 2 non-mycobacterial *Actinobacteria* (*Nocardia farcinica* and *Gordonia bronchialis*) genomes that were selected as out-group species (Supplementary tables S1-S3).

Interestingly, this approach identified ESX loci not only in numerous chromosomal segments (Supplementary table S1), but also revealed ESX motifs in 13 plasmids listed in the NCBI database (Table 1), ranging from 97 kb to 615 kb in size. One of these plasmids corresponded to the recently described *M. marinum* pRAW plasmid harbouring an ESX-P1 system (Ummels, *et al.* 2014). In addition, one isolate from our clinical strain collection, named *M. abscessus subsp. bolletii* strain 5625 was found to contain three distinct ESX loci. When we aligned the contig sequences from this strain to the *M. abscessus* reference genome (Ripoll, *et al.* 2009) and sorted the contigs based on to alignment or lack of such, a clear distinction was noticed. Within the group of the contig sequences aligning to the reference, the sequences were identical to the ESX-3 and ESX-4 systems of the *M. abscessus* reference genome. In contrast, within the non-aligned contig sequences, we noticed a new ESX locus that differed substantially from the known ESX-3 and ESX-4 systems of *M. abscessus*. To evaluate whether this latter locus was of plasmid origin, we prepared highly concentrated genomic DNA from strain 5625 and subjected it to PFGE analysis and Southern hybridization using a specific probe from the non-aligning ESX sequences. As shown in Figure 1, PFGE analysis of non-digested genomic DNA from this strain revealed a band of ca. 100 kb that hybridized with the specific ESX probe. In agreement with previous observations reported for *Mycobacterium ulcerans* strains (Stinear, *et al.* 2004), linearized forms of large, circular plasmids do migrate in PFGE gels, opposed to high molecular weight chromosomal DNA that remains immobilized in the wells. This example of strain 5625 shown in Figure 1 thus serves as a proof of concept that ESX clusters identified by motif search in genome sequence databases may indeed be localized on large plasmids of mycobacterial species or strains. The plasmid in *M. abscessus subsp. bolletii* strain 5625 was named pMBOL. Overall, this information is also important for confirmation of the aforementioned results from NCBI database motif search, which identified 13 new, apparently plasmid-encoded ESX systems (Table 1, Figure 2A and Supplementary table S3) that are the main subject of our here presented study.

Mycobacterial ESX diversity

In parallel to our motif search-based analysis, manual gene annotation was applied to chromosomal ESX-loci of selected, representative species (*M. abscessus*, *M. sp. 960*, *M. mageritense*, *M. sinense JDM601*, *M. marinum*, and *M. tuberculosis*, respectively belonging to three different RGM groups, to the intermediate *M. terrae* complex group, and to two different SGM groups) and two closely related actinobacterial outgroups (*N. farcinica*, and *G. bronchialis*) (Figure 2B). This screening showed that most ESX systems identified in the different mycobacteria and actinobacterial outgroups as being of chromosomal origin, displayed similarities in gene order and gene content with the previously described ESX types of *M. tuberculosis* (Bitter, *et al.* 2009). However, this analysis also identified an additional, novel ESX variant in the chromosomal sequences of *M. sp. 960*, and *M. mageritense,* which showed some resemblance to ESX-4 systems and was termed ESX-4-bis (Figure 2B). The distinction between ESX-4-bis and classical ESX-4 was made on criteria concerning gene order and gene orientation. Whereas mycobacterial ESX-4 systems show a typical *eccB*/*mycP*/*eccD*/*eccC*/*esx* gene order, ESX-4-bis profiles contain two variants of EccD-encoding genes, situated up and downstream of *eccC*, displaying a yet unknown *eccE*/*eccB*/*eccD*/*eccC*/*eccD*/*mycP* gene order. Strikingly, ESX-4-bis loci, similar to ESX-4 systems, lacked PE/PPE encoding genes and *espG* genes, whose gene products were reported to interact and play important roles in the biology of mycobacteria (Bottai, *et al.* 2011; Ekiert and Cox 2014; Korotkova, *et al.* 2014).

From all identified ESX types, the ESX-4 systems were the most widely distributed ESX system in mycobacterial species (Supplementary table S1), which is in agreement with previous reports (Tekaia, *et al.* 1999; Gey Van Pittius, *et al.* 2001). Other systems, such as ESX-1 and ESX-3 systems were also widely present in diverse species, whereas ESX-2 and ESX-5 systems were restricted to the SGM and *M. terrae* complex subgroups, in accordance with data in the literature (Gey van Pittius, *et al.* 2006; Bitter, *et al.* 2009; Bottai, *et al.* 2014).

When the aforementioned plasmid-encoded ESX clusters were subjected to manual annotation, several novel ESX gene-organization profiles were found (Figure 2A, Supplementary table S2), which could be regrouped in ESX-P clusters or represented singletons (Figure 2A). Interestingly, members of ESX-P cluster 1 were present in plasmids from SGM species *M. marinum*, *Mycobacterium kansasii* and *Mycobacterium yongonense*, whereas members of ESX-P clusters 2, 3 and 4 or singletons were found in plasmids from various RGM species (Figure 2A).

Classification and phylogeny of ancestral and mycobacteria-specific ESX types

In order to define the similarity/distance of these new ESX systems relative to the 5 classical chromosomal ESX-1-2-3-4-5 types, we reconstructed the individual phylogenies of selected ESX proteins, namely the ESX-conserved-components EccB and EccC (Bitter, *et al.* 2009), as well as the MycP protease across the different mycobacterial species. Comparison of their amino acid sequences revealed that EccB, EccC and MycP proteins from different species formed distinct clusters, in which orthologous proteins of each of the 5 chromosomal ESX types were grouped together, in agreement with the current ESX classification scheme (Supplementary figure S1) (Gey Van Pittius, *et al.* 2001; Bitter, *et al.* 2009). Moreover, within each ESX type, the ESX protein-based phylogeny was found to be congruent with the mycobacterial species-based phylogeny, separating RGM and SGM within ESX clusters ESX-4-3-1 into different sub-clades (Supplementary figure S1). The results further showed that ESX-4 and ESX-3 systems are ubiquitously distributed within the genus *Mycobacterium*, present in almost all RGM and SGM species analysed. Moreover, ESX-1 systems were also frequently found both in SGM and a subgroup of RGM species. In contrast, the remaining two chromosomal ESX systems (ESX-2 and ESX-5) showed a more restricted distribution. ESX-5 systems were present exclusively in SGM and *M. terrae* complex species, whereas ESX-2 systems were restricted to one particular sub-group of the SGM and *M. terrae* complex. The characteristic gene order in each ESX-cluster (Figure 2B), the similar phylogenetic clustering of each of the three tested proteins (Supplementary figure S1), together with the results from the Approximately Unbiased test (AU test) of phylogenetic tree selection (Supplementary figure S2), suggest that the ESX loci are encoded by stably associated blocks of homologous genes. These findings encouraged us to concatenate the EccB, EccC and MycP sequences with the aim to calculate a global phylogeny of ESX loci and to investigate the long-term evolutionary relationships among the different ESX types.

In the phylogenetic tree obtained (Figure 3), the chromosomal ESX-1-ESX-5 loci form the major branches supported by bootstrap values ranging from 99 to 100%. As seen for the analysis of the single EccB/C or MycP proteins, the branches of ESX-4, ESX-3 and ESX-1 are sub-divided into systems from RGM and SGM species. The concatenated sequence-based tree (Figure 3), together with the AU test (Supplementary figure S2), also supports the monophyletic relationship of the mycobacterial ESX-4 and ESX-4-bis systems, with the non-mycobacterial actinobacterial ESX-4-like systems from *N. farcinica*, and *G. bronchialis*. Indeed, the ESX-4 associated types were clearly separated from the other, mycobacteria-specific chromosomal and plasmid-borne ESX types (bootstrap value 100%), emphasizing the ancestral character of ESX-4 and ESX-4-bis systems. Interestingly, several mycobacterial strains harboured both a classical ESX-4 system and an ESX-4-bis system (Figure 3). Moreover, our phylogenetic analysis revealed that ESX-1 and ESX-3 systems each formed clearly separated clusters with little intra-cluster diversity, whereas the ESX-5 and ESX-2 clusters share a common root and thus form a subgroup within the proposed phylogeny. However, the most interesting novel insights from the study come from inspection of the plasmid borne ESX-systems, which branch at deep rooting positions next to the ESX-1, ESX-3 and ESX-2-5 systems (described in further detail below).

Classification of plasmid-borne ESX families (ESX-P)

Analysis of the data presented in the phylogenetic tree of ESX concatenated sequences showed that the different ESX-P types are grouping together with certain chromosomal ESX families (Figure 3 and Supplementary figure S2). Members of the ESX-P cluster 4, for example, were found to group together with the ESX-3 family (bootstrap value 99%, confirmed by AU test). Two consecutively branching groups, constituted by members of ESX-P clusters 2 and 3 were found at the root of the chromosomal ESX-2 types (bootstrap values 95% and 98% respectively). Moreover, the members of the ESX-P cluster 1 branched at the root of the ESX-5 systems (bootstrap value 100%) (Figure 3 and Supplementary figure S2). Each ESX-P cluster was characterised by a specific gene organization. However, all plasmid-borne ESX types shared a minimal common gene order defined by *eccC*/*PE*/*PPE*/*esx*/*esx* and *eccD*/*mycP*/*eccE*. Interestingly, the gene order in ESX-P profiles differed markedly from ancestral ESX types and was closer to the ESX-2, ESX-3 and ESX-5 organisation, which also showed an *eccD*/*mycP*/*eccE* organization.

Finally, the distribution of the different ESX systems on the phylogenetic tree also allowed us to classify two yet non-classified ESX clusters that were found on non-aligned contigs from *M. aromaticivorans and M. triplex*. These sequences grouped with ESX-P clusters 1 and 4, respectively (Figure 3, dotted red circles and Supplementary figure S2) and also shared similar genetic organisation containing both elements of type IV and type VII secretion systems (Supplementary figures S3 and S4), suggesting that they might represent yet unknown plasmid-borne ESX systems.

To exclude that branches supporting the different plasmid-borne ESX families, which are located between chromosomal ESX groups were the result of genetic mosaicism and recombination between chromosomal ESX systems, we analysed our dataset using the Recombination Detection Program RDP4 (Martin, *et al.* 2015). No recombination events between the chromosomal ESX and plasmid-borne ESX-P systems were detected, limiting the possibility of an artefact due to mosaic ESX genes to a minimum. Moreover, in order to see if plasmid-borne ESX-P clusters were under purifying selection, we calculated the ratios of synonymous and non-synonymous substitutions (Supplementary figure S5). This analysis showed that EccB, EccC, and MycP encoding genes from ESX-P clusters 1, 2 and 3 were under purifying selection (dn/ds<1). This result advocates for a diversification process leading to the observed ESX-P diversity (rather than lack of selection pressure leading to various degenerated ESX systems). Taken together, all these data suggest that ESX-P systems represent genuine functional and diversified, plasmid-specific ESX families.

Finally, the gene order within the various ESX-P systems was also consistent in most cases with the phylogeny obtained from concatenated sequences (Figures 2A and 3). Similarly to ESX-P cluster 4, in ESX-1 and ESX-3 the position of *eccA* was found to be located at the upstream part of the ESX locus, followed by *eccB/eccC*. On the contrary, in chromosomal ESX-2 and ESX-5 systems EccA is encoded in the most downstream part of the ESX locus, after *eccD/mycP/eccE*, a constellation, which is also observed in the plasmid-borne ESX-P clusters 1-2-3. These similarities are consistent with the ESX-P positions within the distance tree based on concatenated sequences (Figure 3) and thus suggest a plausible evolutionary link between ESX-P cluster 4 and ESX-3/ESX-1 on the one side, as well as ESX-P clusters 1-2-3 and ESX-2/ESX-5 on the other side.

Phylogeny of ESX-P families and mycobacteria-specific genomic ESX

To investigate the evolutionary history of plasmid-borne and chromosomal mycobacteria-specific ESX systems we performed synteny analysis of the ESX loci using the Microbial Genome Annotation & Analysis Platform MaGe (Vallenet, *et al.* 2009). This tool was used to determine synteny blocks in the vicinity of ESX-P loci. In all investigated ESX-encoding plasmids, ESX loci were embedded within larger synteny blocks including plasmid-specific type IV secretion system genetic elements, such as genes encoding VirD4, TrpC, and VirB4 (Figure 4A and Supplementary figures S3 and S4). Within the different plasmids, ESX-P and Type-IV loci were contiguous, and displayed various relative positions probably due to plasmid rearrangements. The observation of these large synteny blocks involving both ESX and type IV systems strongly support that ESX-P systems are phylogenetically related. The ESX-encoding plasmids thus form a group that seems to derive from a single common origin. Variation of gene order most probably diversified through plasmid rearrangements. Moreover, the observation of the *eccA* position within the various clusters suggests that this gene co-migrates with type IV genetic rearrangements. Thus, the differences observed in *eccA* positions among the various ESX-P clusters might be explained by these local rearrangements. Interestingly, as explained above, the position of *eccA* is a feature that differentiates ESX-1/ESX-3 from ESX-2/ESX-5 systems. Thus, plasmid rearrangements may have made a phylogenetic link between these genomic ESX systems, suggesting that diversification of ESX-coding plasmids might be at the origin of –at least some- mycobacteria-specific chromosomal ESX types. This hypothesis is consistent with observed phylogeny, showing ESX-P systems branching at the root of mycobacteria-specific chromosomal ESX systems (Figure 3). Such scenario would thus necessitate a chromosomal integration of ESX-P systems through horizontal gene transfer (HGT) into mycobacteria.

Clues of horizontal gene transfer between ESX-P and genomic ESX

In order to investigate further the hypothesis of a plasmid-borne origin of mycobacteria-specific chromosomal ESX systems, we focused on ESX-2 and ESX-5. These ESX systems are absent from RGM and present in SGM and *M. sinense* JDM601 (a species that belongs to the intermediate group of the *Mycobacterium terrae* complex). Interestingly, genomic comparison and synteny analysis of the ESX-2 locus in *M. sinense* JDM601 showed that this gene cluster is embedded into a larger synteny block which is present in SGM chromosomes and ESX-encoding plasmids pMKMS01 and pMYCCH02 of the RGM species *M. sp* KMS and *M. chubuense,* respectively, whereas it is absent from RGM chromosomes (Figure 4B). Interestingly, this synteny block harbours a gene bearing an NLP/p60 domain, which is found in most ESX-P systems (Supplementary table S4), and which is involved in *B. subtilis* conjugation functions (DeWitt and Grossman 2014). The synteny block also contained a gene encoding BssS, a biofilm regulator that has homologs only in ESX-2 loci and in mycobacterial plasmids (Supplementary table S5). Taken together, these findings may serve as one example how a chromosomal ESX system might have emerged by genetic exchange that apparently occurred between ESX-encoding plasmids and mycobacterial chromosomes.

To identify putative regions of exogenous DNA integration, specific for SGM and members of the *M. terrae* complex (that specifically contained ESX-2 and ESX-5), we used the MaGe platform (Vallenet, *et al.* 2009) to find regions of genomic plasticity. Selection criteria for members of these regions were the following: *M. tuberculosis* H37Rv genes should share homologs in both *M. avium* and *M. sinense* JDM601 but without any homolog in *M. smegmatis*, *M. gilvum* PYR-GCK and *M. abscessus* (best bidirectional hit with 30% identity threshold). Furthermore, the selected genes should also be present within a synteny group showing compositional bias (Vernikos and Parkhill 2006), as identified by the Alien Hunter software (Figure 5A). Interestingly, ESX-2 and

ESX-5 were both found in genomic regions that were detected as regions of genomic plasticity (Figure 5A). Moreover, the putative genomic island region flanking ESX-5 also contained mobile genetic elements, such as insertion sequences as well as tRNA genes known to serve as potential integration sites (Figure 5A). Moreover, this ESX system was found to be embedded within a larger 50 kb synteny block present in SGM and *M. terrae* complex species, but absent from all tested RGM species (Figure 5B). Taken together, these findings support the hypothesis that ESX-2 and ESX-5 might have been acquired by SGM and *M. terrae* complex species via independent horizontal gene transfer (HGT) episodes during mycobacterial evolution, most probably from ESX-encoding plasmids.

Discussion

Gene flow is an important factor of bacterial niche adaptation and speciation through the acquisition of foreign genetic material by HGT. The mechanisms that mediate this process comprise phage transduction, natural transformation, and plasmid conjugation, and these events are especially important for the transfer of antibiotic resistance and acquisition of virulence factors (Blair, *et al.* 2015). However, for mycobacteria the impact of HGT in the pathogenomic evolution of its members remains largely unknown. Some insights have been gained from the analysis of genomic islands in the genome of *M. tuberculosis* (Rosas-Magallanes, *et al.* 2006; Becq, *et al.* 2007), but the question remains how in the earlier evolution of the pathogenic SGM species HGT might have been organized and by which mechanisms gene flow was enabled to occur. In many bacterial species, transfer of plasmids is one of the key driving forces of HGT. For mycobacteria, it is known for long time that plasmids are present in some species (Le Dantec, *et al.* 2001; Stinear, *et al.* 2004; Stinear, *et al.* 2008; Ripoll, *et al.* 2009; Leao, *et al.* 2013; Uchiya, *et al.* 2015), although the classical OriT/type IV conjugative systems do not seem to play a role in this genus. However, recent experiments showed that conjugal transfer of plasmids can be observed in certain *M. marinum* strains, involving a novel type of conjugative plasmid that possesses an ESX system and elements of a classical type IV system, located on the same plasmid, named pRAW (Ummels, *et al.* 2014). The identification of this plasmid-mediated conjugation mechanism is supported by a previous report that described a putative plasmid transfer between the SGM species *M. avium* and *M. kansasii* in a mixed infection in a patient (Rabello, *et al.* 2012). Apart from these rare reports on HGT mediated by plasmids, it is also known that mycobacterial HGT may be organized via chromosomally encoded conjugation systems. This is the case for a process driven by the ESX-1 system of *M. smegmatis,* resulting in genome-wide recombination clusters and mosaicism that was named distributive conjugal transfer (Gray, *et al.* 2013). Together, the examples presently described in the literature suggest that conjugative processes might have been - or still are - responsible for certain episodes of HGT among mycobacterial strains, thereby driving mycobacterial evolution. However, it should also be mentioned that overall, the insights into the mechanisms of HGT and gene flow in mycobacteria are scarce, which was one of the main motivations for us to undertake this study and use recently available mycobacterial pan genome data to elucidate the question of potential mobile conjugation systems and HGT in mycobacteria.

This analysis allowed us to explore the diversity and the putative origin of ESX systems in mycobacterial chromosomes and plasmids. Our approach confirmed that the five previously designated chromosomal ESX types (ESX-1-5) (Gey Van Pittius, *et al.* 2001; Bitter, *et al.* 2009) constitute meaningful groups from a phylogenetic point of view, since they represent well-defined phylogenetic clusters, each of them being in accordance with mycobacterial phylogeny. We also confirmed the ancestral nature of the ESX-4 type, and identified novel ESX-4 like type, named ESX-4-bis, which were present in various mycobacterial strains in addition to the classical ESX-4 systems.

Importantly, our analysis resulted in the identification of new, divergent ESX systems encoded on plasmids, thereby largely expanding the current knowledge on ESX-type diversity. The description of new genetic ESX organization-schemes in mycobacterial mega-plasmids (>100kb) suggests that, besides the well-known type VII secretion system functions, *i.e.* pathogenicity, metal ion uptake, and conjugation, other yet unknown functions may potentially be provided by these yet unexplored ESX systems. In addition, their location on mega-plasmids with large coding capacities suggests that the presence of ESX-carrying plasmids in selected strains might modulate the phenotype of the concerned mycobacteria, and thus might be an important factor for promoting niche adaptation in new environments. In a more practical perspective, the identification of a 100 kb sized plasmid pMBOL in *M. abscessus subsp. bolletii* strain now provides the possibility for experimentally addressing such questions on evolution and transfer of ESX-containing plasmids and the involved mechanisms.

During data analysis and the generation of the phylogenetic tree (Figure 3), the question arose whether our analysis could have been biased by genetic saturation and "long branch attraction" phenomena (Philippe and Forterre 1999; Raymann, *et al.* 2015), as for the comparison of distantly-related ESX types such effects cannot be excluded *a priori*. However, we are confident that these phenomena did not have a measurable impact on the results of our analysis because several other characteristics such as AU test results, gene order, synteny and lacking gene sequence mosaicisms in different ESX clusters also support the obtained phylogeny. Based on this converging body of evidence an evolutionary scenario can be proposed in which ancestral ESX-4-like systems present in mycobacteria and/or other actinobacterial species had been transferred onto plasmids, and underwent extensive rearrangement processes, leading to diverse forms of new ESX types. Some of these rearranged ESX types were subsequently transferred to the chromosomes of certain mycobacteria, resulting in the mycobacteria-specific ESX types. Since ESX-5 and ESX-2 are found exclusively in SGM and *M. terrae* complex species (*M. sinense* JDM601), their putative chromosomal acquisition by HGT seems to have occurred in episodes prior or during SGM differentiation. It is tempting to hypothesize that some HGT episodes like for example the acquisition of ESX-5 might have contributed to acquisition of new functions to SGM species that are now exploited by pathogenic SGM species during host-pathogen interaction (Abdallah, *et al.* 2011; Bottai, *et al.* 2012; Sayes, *et al.* 2012; Ates, *et al.* 2015).

In conclusion, our study provides new insights on the diversity and conservation of ESX systems in a broad range of mycobacteria and proposes a unique model in which ESX-carrying plasmids play a key role in the distribution and refinement of type VII secretion-related processes during the long-term evolution of the mycobacterial genus. As observed from the different ESX-related gene distribution profiles, the involved plasmids might not only have acted as mycobacterial gene-exchange vectors, but might also have served as accelerators of adaptation and biodiversity with probable impact on the emergence of mycobacterial pathogenicity.

Competing interests

The authors declare that they have no competing interests.

Authors' contributions

ED and GS designed the study. RB, JLG, FGM, RCRV and BH supplied material and expertise; MV, JMT and VC performed genome sequencing. ED, ECB and FGM undertook experiments, ED and GS performed genome and phylogenetic analyses. RB, ED and GS wrote the manuscript with contributions from all authors. All authors approved the final manuscript.

Acknowledgements

We are grateful to Guillaume Achaz, Sophie Brouillet, Joël Pothier (Atelier de Bioinformatique de Jussieu), Philippe Lopez (UMR 7138 – Université Pierre et Marie Curie) and to Jean-Louis Herrmann (INSERM U1173, UFR Simone Veil, Versailles-Saint-Quentin University) for help and advice. We acknowledge the support by the European Community's grants 260872 and H2020-PHC-643381, and the Fondation pour la Recherche Médicale FRM (DEQ20130326471). E.C.B.

was supported by a stipend from the Pasteur–Paris University (PPU) International PhD program and the Institut Carnot Pasteur Maladies Infectieuses.

Literature Cited

Abascal F, Zardoya R, Posada D. 2005. ProtTest: selection of best-fit models of protein evolution. Bioinformatics. 21:2104-2105.

Abascal F, Zardoya R, Telford MJ. 2010. TranslatorX: multiple alignment of nucleotide sequences guided by amino acid translations. Nucleic Acids Res. 38:W7-13.

Abdallah AM, Bestebroer J, Savage ND, de Punder K, van Zon M, Wilson L, Korbee CJ, van der Sar AM, Ottenhoff TH, van der Wel NN, *et al.* 2011. Mycobacterial secretion systems ESX-1 and ESX-5 play distinct roles in host cell death and inflammasome activation. J Immunol 187:4744-4753.

Abdallah AM, Gey van Pittius NC, Champion PA, Cox J, Luirink J, Vandenbroucke-Grauls CM, Appelmelk BJ, Bitter W. 2007. Type VII secretion system of mycobacteria show the way. Nat Rev Microbiol 5:883-891.

Abdallah AM, Verboom T, Weerdenburg EM, Gey van Pittius NC, Mahasha PW, Jimenez C, Parra M, Cadieux N, Brennan MJ, Appelmelk BJ, *et al.* 2009. PPE and PE_PGRS proteins of *Mycobacterium marinum* are transported via the type VII secretion system ESX-5. Mol Microbiol 73:329-340.

Altschul S, Gish W, Miller W, Myers E, Lipman D. 1990. A basic local alignment search tool. J. Mol. Biol. 215:403-410.

Ates LS, Ummels R, Commandeur S, van der Weerd R, Sparrius M, Weerdenburg E, Alber M, Kalscheuer R, Piersma SR, Abdallah AM, *et al.* 2015. Essential role of the ESX-5 secretion system in outer membrane permeability of pathogenic mycobacteria. PLoS Genet. 11:e1005190.

Becq J, Gutierrez MC, Rosas-Magallanes V, Rauzier J, Gicquel B, Neyrolles O, Deschavanne P. 2007. Contribution of horizontally acquired genomic islands to the evolution of the tubercle bacilli. Mol Biol Evol 24:1861-1871.

Behr MA, Wilson MA, Gill WP, Salamon H, Schoolnik GK, Rane S, Small PM. 1999. Comparative genomics of BCG vaccines by whole-genome DNA microarray. Science 284:1520-1523.

Besemer J, Borodovsky M. 2005. GeneMark: web software for gene finding in prokaryotes, eukaryotes and viruses. Nucleic Acids Res. 33:W451-454.

Bitter W, Houben EN, Bottai D, Brodin P, Brown EJ, Cox JS, Derbyshire K, Fortune SM, Gao LY, Liu J, *et al.* 2009. Systematic genetic nomenclature for type VII secretion systems. PLoS Pathog 5:e1000507.

Blair JM, Webber MA, Baylay AJ, Ogbolu DO, Piddock LJ. 2015. Molecular mechanisms of antibiotic resistance. Nat Rev Microbiol. 13:42-51.

Boritsch EC, Supply P, Honore N, Seemann T, Stinear TP, Brosch R. 2014. A glimpse into the past and predictions for the future: the molecular evolution of the tuberculosis agent. Mol Microbiol. 93:835-852.

Bottai D, Di Luca M, Majlessi L, Frigui W, Simeone R, Sayes F, Bitter W, Brennan MJ, Leclerc C, Batoni G, *et al.* 2012. Disruption of the ESX-5 system of *Mycobacterium tuberculosis* causes loss of PPE protein secretion, reduction of cell wall integrity and strong attenuation. Mol Microbiol 83:1195-1209.

Bottai D, Majlessi L, Simeone R, Frigui W, Laurent C, Lenormand P, Chen J, Rosenkrands I, Huerre M, Leclerc C, *et al.* 2011. ESAT-6 secretion-independent impact of ESX-1 genes *espF* and *espG$_1$* on virulence of *Mycobacterium tuberculosis*. J Infect Dis 203:1155-1164.

Bottai D, Stinear TP, Supply P, Brosch R. 2014. Mycobacterial Pathogenomics and Evolution Microbiol Spectrum 2:MGM2-0025-2013

Brodin P, Rosenkrands I, Andersen P, Cole ST, Brosch R. 2004. ESAT-6 proteins: protective antigens and virulence factors? Trends Microbiol 12:500-508.

Brosch R, Gordon SV, Buchrieser C, Pym AS, Garnier T, Cole ST. 2000. Comparative genomics uncovers large tandem chromosomal duplications in *Mycobacterium bovis* BCG Pasteur. Yeast 17:111-123.

Carver TJ, Rutherford KM, Berriman M, Rajandream MA, Barrell BG, Parkhill J. 2005. ACT: the Artemis Comparison Tool. Bioinformatics 21:3422-3423.

Cole ST, Brosch R, Parkhill J, Garnier T, Churcher C, Harris D, Gordon SV, Eiglmeier K, Gas S, Barry CE, 3rd, *et al.* 1998. Deciphering the biology of *Mycobacterium tuberculosis* from the complete genome sequence. Nature 393:537-544.

Coros A, Callahan B, Battaglioli E, Derbyshire KM. 2008. The specialized secretory apparatus ESX-1 is essential for DNA transfer in *Mycobacterium smegmatis*. Mol Microbiol 69:794-808.

Delcher AL, Phillippy A, Carlton J, Salzberg SL. 2002. Fast algorithms for large-scale genome alignment and comparison. Nucleic Acids Res 30:2478-2483.

Dereeper A, Guignon V, Blanc G, Audic S, Buffet S, Chevenet F, Dufayard JF, Guindon S, Lefort V, Lescot M, *et al.* 2008. Phylogeny.fr: robust phylogenetic analysis for the non-specialist. Nucleic Acids Res. 36:W465-469.

DeWitt T, Grossman AD. 2014. The bifunctional cell wall hydrolase CwlT is needed for conjugation of the integrative and conjugative element ICEBs1 in *Bacillus subtilis* and *B. anthracis*. J Bacteriol. 196:1588-1596.

Ekiert DC, Cox JS. 2014. Structure of a PE-PPE-EspG complex from *Mycobacterium tuberculosis* reveals molecular specificity of ESX protein secretion. Proc Natl Acad Sci U S A. 111:14758-14763.

Finn RD, Clements J, Eddy SR. 2011. HMMER web server: interactive sequence similarity searching. Nucleic Acids Res. 39:W29-37.

Gey Van Pittius NC, Gamieldien J, Hide W, Brown GD, Siezen RJ, Beyers AD. 2001. The ESAT-6 gene cluster of *Mycobacterium tuberculosis* and other high G+C Gram-positive bacteria. Genome Biol 2:RESEARCH0044.

Gey van Pittius NC, Sampson SL, Lee H, Kim Y, van Helden PD, Warren RM. 2006. Evolution and expansion of the *Mycobacterium tuberculosis* PE and PPE multigene families and their association with the duplication of the ESAT-6 (esx) gene cluster regions. BMC Evol Biol 6:95.

Gray TA, Krywy JA, Harold J, Palumbo MJ, Derbyshire KM. 2013. Distributive conjugal transfer in mycobacteria generates progeny with meiotic-like genome-wide mosaicism, allowing mapping of a mating identity locus. PLoS Biol 11:e1001602.

Guindon S, Dufayard JF, Lefort V, Anisimova M, Hordijk W, Gascuel O. 2010. New algorithms and methods to estimate maximum-likelihood phylogenies: assessing the performance of PhyML 3.0. Syst Biol. 59:307-321.

Houben D, Demangel C, van Ingen J, Perez J, Baldeon L, Abdallah AM, Caleechurn L, Bottai D, van Zon M, de Punder K, *et al.* 2012. ESX-1-mediated translocation to the cytosol controls virulence of mycobacteria. Cell Microbiol 14:1287-1298.

Kaur D, Guerin ME, Skovierova H, Brennan PJ, Jackson M. 2009. Chapter 2: Biogenesis of the cell wall and other glycoconjugates of *Mycobacterium tuberculosis*. Adv Appl Microbiol 69:23-78.

Kim BJ, Kim BR, Hong SH, Seok SH, Kook YH, Kim BJ. 2013. Complete genome sequence of *Mycobacterium massiliense* clinical strain Asan 50594, belonging to the type II genotype. Genome Announc. 1(4).e00429-00413.

Kim BJ, Kim BR, Lee SY, Seok SH, Kook YH, Kim BJ. 2013. Whole-Genome sequence of a novel species, *Mycobacterium yongonense* DSM 45126T. Genome Announc. 1(4).e00604-00613.

Koressaar T, Remm M. 2007. Enhancements and modifications of primer design program Primer3. Bioinformatics. 23:1289-1291.

Korotkova N, Freire D, Phan TH, Ummels R, Creekmore CC, Evans TJ, Wilmanns M, Bitter W, Parret AH, Houben EN, *et al.* 2014. Structure of the *Mycobacterium tuberculosis* type VII secretion system chaperone EspG5 in complex with PE25-PPE41 dimer. Mol Microbiol. 94:367-382.

Le Chevalier F, Cascioferro A, Majlessi L, Herrmann JL, Brosch R. 2014. *Mycobacterium tuberculosis* evolutionary pathogenesis and its putative impact on drug development. Future Microbiol. 9:969-85.:10.2217/fmb.2214.2270.

Le Dantec C, Winter N, Gicquel B, Vincent V, Picardeau M. 2001. Genomic sequence and transcriptional analysis of a 23-kilobase mycobacterial linear plasmid: evidence for horizontal transfer and identification of plasmid maintenance systems. J Bacteriol. 183:2157-2164.

Leao SC, Matsumoto CK, Carneiro A, Ramos RT, Nogueira CL, Lima JD, Jr., Lima KV, Lopes ML, Schneider H, Azevedo VA, *et al.* 2013. The detection and sequencing of a broad-host-range conjugative IncP-1beta plasmid in an epidemic strain of *Mycobacterium abscessus* subsp. *bolletii*. PLoS One 8:e60746.

Letunic I, Bork P. 2011. Interactive Tree Of Life v2: online annotation and display of phylogenetic trees made easy. Nucleic Acids Res. 39:W475-478.

Magee JG, Ward AC. 2012. Genus I. *Mycobacterium*. In: Goodfellow M, Kämpfer P, Busse HJ, Trujillo ME, Suzuki KI, Ludwig W, Whitman WB, editors. Bergey's Manual of Systematic Bacteriology, The *Actinobacteria*. New York,: Springer. p. 312-375.

Mahairas GG, Sabo PJ, Hickey MJ, Singh DC, Stover CK. 1996. Molecular analysis of genetic differences between *Mycobacterium bovis* BCG and virulent *M. bovis*. J Bacteriol 178:1274-1282.

Majlessi L, Prados-Rosales R, Casadevall A, Brosch R. 2015. Release of mycobacterial antigens. Immunol Rev. 264:25-45.

Martin DP, Murrell B, Golden M, Khoosal A, Muhire B. 2015. RDP4: Detection and analysis of recombination patterns in virus genomes. Virus Evolution 1:vev003.

Mignard S, Flandrois JP. 2008. A seven-gene, multilocus, genus-wide approach to the phylogeny of mycobacteria using supertrees. Int J Syst Evol Microbiol. 58:1432-1441.

Mortimer TD, Pepperell CS. 2014. Genomic signatures of distributive conjugal transfer among mycobacteria. Genome Biol Evol. 6:2489-2500.

Philippe H, Forterre P. 1999. The rooting of the universal tree of life is not reliable. J Mol Evol. 49:509-523.

Pym AS, Brodin P, Brosch R, Huerre M, Cole ST. 2002. Loss of RD1 contributed to the attenuation of the live tuberculosis vaccines *Mycobacterium bovis* BCG and *Mycobacterium microti*. Mol Microbiol 46:709-717.

Rabello MC, Matsumoto CK, Almeida LG, Menendez MC, Oliveira RS, Silva RM, Garcia MJ, Leao SC. 2012. First description of natural and experimental conjugation between mycobacteria mediated by a linear plasmid. PLoS One 7:e29884.

Raymann K, Brochier-Armanet C, Gribaldo S. 2015. The two-domain tree of life is linked to a new root for the *Archaea*. Proc Natl Acad Sci U S A. 112:6670-6675.

Ripoll F, Pasek S, Schenowitz C, Dossat C, Barbe V, Rottman M, Macheras E, Heym B, Herrmann JL, Daffe M, *et al.* 2009. Non mycobacterial virulence genes in the genome of the emerging pathogen *Mycobacterium abscessus*. PLoS One 4:e5660.

Rosas-Magallanes V, Deschavanne P, Quintana-Murci L, Brosch R, Gicquel B, Neyrolles O. 2006. Horizontal transfer of a virulence operon to the ancestor of *Mycobacterium tuberculosis*. Mol Biol Evol. 23:1129-1135.

Sayes F, Sun L, Di Luca M, Simeone R, Degaiffier N, Fiette L, Esin S, Brosch R, Bottai D, Leclerc C, *et al.* 2012. Strong immunogenicity and cross-reactivity of *Mycobacterium tuberculosis* ESX-5 Type VII Secretion- encoded PE-PPE proteins predicts vaccine potential. Cell Host Microbe 11:352-363.

Schmidt HA, Strimmer K, Vingron M, von Haeseler A. 2002. TREE-PUZZLE: maximum likelihood phylogenetic analysis using quartets and parallel computing. Bioinformatics. 18:502-504.

Serafini A, Boldrin F, Palu G, Manganelli R. 2009. Characterization of a *Mycobacterium tuberculosis* ESX-3 conditional mutant: essentiality and rescue by iron and zinc. J Bacteriol 191:6340-6344.

Shimodaira H, Hasegawa M. 2001. CONSEL: for assessing the confidence of phylogenetic tree selection. Bioinformatics. 17:1246-1247.

Siegrist MS, Steigedal M, Ahmad R, Mehra A, Dragset MS, Schuster BM, Philips JA, Carr SA, Rubin EJ. 2014. Mycobacterial Esx-3 requires multiple components for iron acquisition. MBio 5:e01073-01014.

Simeone R, Sayes F, Song O, Groschel MI, Brodin P, Brosch R, Majlessi L. 2015. Cytosolic access of *Mycobacterium tuberculosis*: Critical impact of phagosomal acidification control and demonstration of occurrence *in vivo*. PLoS Pathog. 11:e1004650.

Stinear TP, Mve-Obiang A, Small PL, Frigui W, Pryor MJ, Brosch R, Jenkin GA, Johnson PD, Davies JK, Lee RE, *et al.* 2004. Giant plasmid-encoded polyketide synthases produce the macrolide toxin of *Mycobacterium ulcerans*. Proc Natl Acad Sci U S A 101:1345-1349.

Stinear TP, Seemann T, Harrison PF, Jenkin GA, Davies JK, Johnson PD, Abdellah Z, Arrowsmith C, Chillingworth T, Churcher C, *et al.* 2008. Insights from the complete genome sequence of *Mycobacterium marinum* on the evolution of *Mycobacterium tuberculosis*. Genome Res 18:729-741.

Supply P, Marceau M, Mangenot S, Roche D, Rouanet C, Khanna V, Majlessi L, Criscuolo A, Tap J, Pawlik A, *et al.* 2013. Genomic analysis of smooth tubercle bacilli provides insights into ancestry and pathoadaptation of *Mycobacterium tuberculosis*. Nat Genet 45:172-179.

Tamura K, Stecher G, Peterson D, Filipski A, Kumar S. 2013. MEGA6: Molecular Evolutionary Genetics Analysis version 6.0. Mol Biol Evol. 30:2725-2729.

Tekaia F, Gordon SV, Garnier T, Brosch R, Barrell BG, Cole ST. 1999. Analysis of the proteome of *Mycobacterium tuberculosis* in silico. Tuber Lung Dis 79:329-342.

Uchiya K, Takahashi H, Nakagawa T, Yagi T, Moriyama M, Inagaki T, Ichikawa K, Nikai T, Ogawa K. 2015. Characterization of a novel plasmid, pMAH135, from *Mycobacterium avium* Subsp. *hominissuis*. PLoS One. 10:e0117797.

Ummels R, Abdallah AM, Kuiper V, Aajoud A, Sparrius M, Naeem R, Spaink HP, van Soolingen D, Pain A, Bitter W. 2014. Identification of a novel conjugative plasmid in mycobacteria that requires both type IV and type VII secretion. MBio. 5:e01744-01714.

Vallenet D, Engelen S, Mornico D, Cruveiller S, Fleury L, Lajus A, Rouy Z, Roche D, Salvignol G, Scarpelli C, *et al.* 2009. MicroScope: a platform for microbial genome annotation and comparative genomics. Database (Oxford) 2009:bap021.

Vernikos GS, Parkhill J. 2006. Interpolated variable order motifs for identification of horizontally acquired DNA: revisiting the *Salmonella* pathogenicity islands. Bioinformatics. 22:2196-2203.

Wallace IM, O'Sullivan O, Higgins DG, Notredame C. 2006. M-Coffee: combining multiple sequence alignment methods with T-Coffee. Nucleic Acids Res. 34:1692-1699.

Wang J, McIntosh F, Radomski N, Dewar K, Simeone R, Enninga J, Brosch R, Rocha EP, Veyrier FJ, Behr MA. 2015. Insights on the emergence of *Mycobacterium tuberculosis* from the analysis of *Mycobacterium kansasii*. Genome Biol Evol. 7:856-870.

Yang Z. 1997. PAML: a program package for phylogenetic analysis by maximum likelihood. Comput Appl Biosci. 13:555-556.

Table 1. General characteristics of the identified mycobacterial ESX-plasmids. GI : identifier from NCBI database. *: publicly released genome sequence without associated publication.

Strain	Plasmid name	Size (kb)	Reference	GI number
I. abscessus subsp. bolletii strain 5625	pMBOL	97	This study	
I. abscessus subsp. bolletii strain 50594	plasmid 2	97	(Kim, Kim, Hong, *et al.* 2013)	506965416
I. chubuense NBB4	pMYCCH.01	615	Lucas, S. *et al.* 2012*	392405727
I. chubuense NBB4	pMYCCH.02	144	Lucas, S. *et al.* 2012*	392406268
I. gilvum PYR-GCK	pMFLV01	321	Copeland, A. *et al.* 2007*	145225871
I. kansasii ATCC 12478	pMK12478	145	(Wang, *et al.* 2015)	556559712
I. marinum E11	pRAW	114	(Ummels, *et al.* 2014)	641308534
I. smegmatis	pMYCSM01	394	Lucas S. *et al.* 2011*	433644115
I. smegmatis	pMYCSM02	199	Lucas S. *et al.* 2011*	433644438
I. smegmatis	pMYCSM03	164	Lucas S. *et al.* 2011*	433644684
I. sp. KMS	pMKMS01	302	Copeland, A. *et al.* 2006*	119854889
I. sp. KMS	pMKMS02	217	Copeland, A. *et al.* 2006*	119855174
I. sp. MCS	plasmid 1	215	Copeland, A. *et al.* 2006*	108772792
I. yongonense 05-1390	pMyong1	123	(Kim, Kim, Lee, *et al.* 2013)	451770451

Figures

Figure 1: Ethidium bromide stained pulsed-field gel electrophoresis (PFGE) gel (left panel) and corresponding Southern hybridization blot (right panel) obtained with a PCR-derived, ^{32}P-labelled probe from ESX-region of *M. bolletii* strain 5625. Lane 1: *M. bolletii* type strain; lane 2: *M. bolletii* 5625. Lane 3: *M. canettii* control strain STB-D (described in (Supply, *et al.* 2013)), lane 4: low-range PFG Marker (NEB). PFGE conditions: 5s ramping to 35s; 6 V/cm; 23h.

Figure 2: Genetic organization of ESX loci. 2A: Genetic organization of ESX-P loci in mycobacterial plasmids. ESX-P clusters 2, 3 and 4 represent new ESX types found in more than one plasmid. 2B: Genetic organization of chromosomal ESX loci from a representative mycobacterial dataset together with *Nocardia farcinica*, and *Gordonia bronchialis* strains. Note that within the ESX-1 locus, the downstream gene of *esxA* was drawn according to the highest coding probability scores, which for *M. tuberculosis* and *M. marinum* were different from the original annotation.

Figure 3: Phylogenetic tree of mycobacterial ESX loci from concatenated sequences of EccB, EccC and MycP. Red circles : plasmid-borne ESX types. Dotted red circles: putative ESX-containing plasmids. Green boxes : *Nocardia farcinica*, and *Gordonia bronchialis*. Best evolution model identified by MEGA software (WAG+G+I). Tree constructed with maximum likelihood method with 250 bootstrap replications. Values >70% are indicated. Note that for some species only selected chromosomal ESX systems are shown, as defined in supplementary table S1, Supplementary Material online. RGM: rapidly growing mycobacteria. SGM: slowly growing mycobacteria.

Figure 4: ESX loci within synteny blocks. Purple arrows : genes involved in synteny block within contiguous region of ESX loci. 4A: synteny blocks involving ESX loci of mycobacterial plasmids from each ESX-P plasmid cluster and *M. gilvum* pMFLV01. 4B: synteny blocks within *M. sinense* JDM601 ESX-2 genomic region. Upper panel: genetic organisation of ESX plasmids pMYCCH02 and pMKMS02 in synteny with *M. sinense* JDM601 ESX-2 locus. Lower panel: a representative subset of slowly and rapidly growing mycobacteria (SGM and RGM respectively) and other closely related actinobacteria were investigated. Blue boxes: synteny blocks. Surrounding purple box: plasmid.

Figure 5: SGM-specific genes of *M. tuberculosis* H37Rv and ESX-5 genomic organisation. A: SGM-specific genes involved in mobility regions. First inner circle: GC%. Second inner circle: red boxes represent *M. tuberculosis* genes with homologs in *M. avium* and *M. sinense* JDM501 but

without any homolog in *M. smegmatis*, *M. gilvum* PYR-GCK, or *M. abscessus* (BBH 30% identity), and identified within synteny groups containing composition bias according to Alien Hunter software. Third inner circle: purple boxes represent ESX loci. First outer circle: tRNAs. Secound outer circle: insertion sequences. B: synteny blocks within ESX-5 region of *M. tuberculosis* H37Rv. A representative subset of slowly and rapidly growing mycobacteria (SGM and RGM respectively) and other closely related actinobacteria were investigated. MTC: *M. terrae* complex. Blue boxes: synteny blocks. Purple box: ESX-5 locus.

Supplementary Material

Supplementary table S1: List of all investigated mycobacterial genomic sequences.

Supplementary table S2: List of studied plasmids.

Supplementary table S3: NCBI reference numbers for the different plasmid-borne ESX-proteins

Supplementary table S4: Type IV elements in ESX plasmids

Supplementary table S5: tblastn results of *Mycobacterium sinense* JDM601 BssS on complete NCBI nucleotide collection.

Supplementary figure S1: Phylogenetic tree of mycobacterial EccB, EccC and MycP. Red branches: plasmid ESX. Green branches : *Nocardia farcinica*, and *Gordonia bronchialis*. For each of the three protein sequence sets, e-values are lower than 10^{-79}, and Gblocks cured alignments represent at least 45% of *M. tuberculosis* homologs. Tree constructed with maximum likelihood method with 250 bootstrap replications. values >80% are indicated. A: EccB; B: EccC; C: MycP. RGM: rapidly growing mycobacteria. SGM: slowly growing mycobacteria.

Supplementary figure S2: Best tree according to the approximately unbiased test of phylogenetic tree selection. Green circles correspond to stable monophyletic groups.

Supplementary figure S3: Artemis Comparison Tool alignment of ESX-P cluster 4 plasmids, against *M. triplex* (scafold NZ_HG964447.1 containing ESX plasmid-like locus). Purple: homologous genomic regions.

Supplementary figure S4: Artemis Comparison Tool alignment of ESX-P cluster 1 plasmids, against *M. aromaticivorans* (contig 2 containing ESX plasmid-like locus). Purple: homologous genomic regions.

Supplementary figure S5: Non-synonymous *vs* synonymous mutations in genomic and plasmid ESX genes.

Figure 1

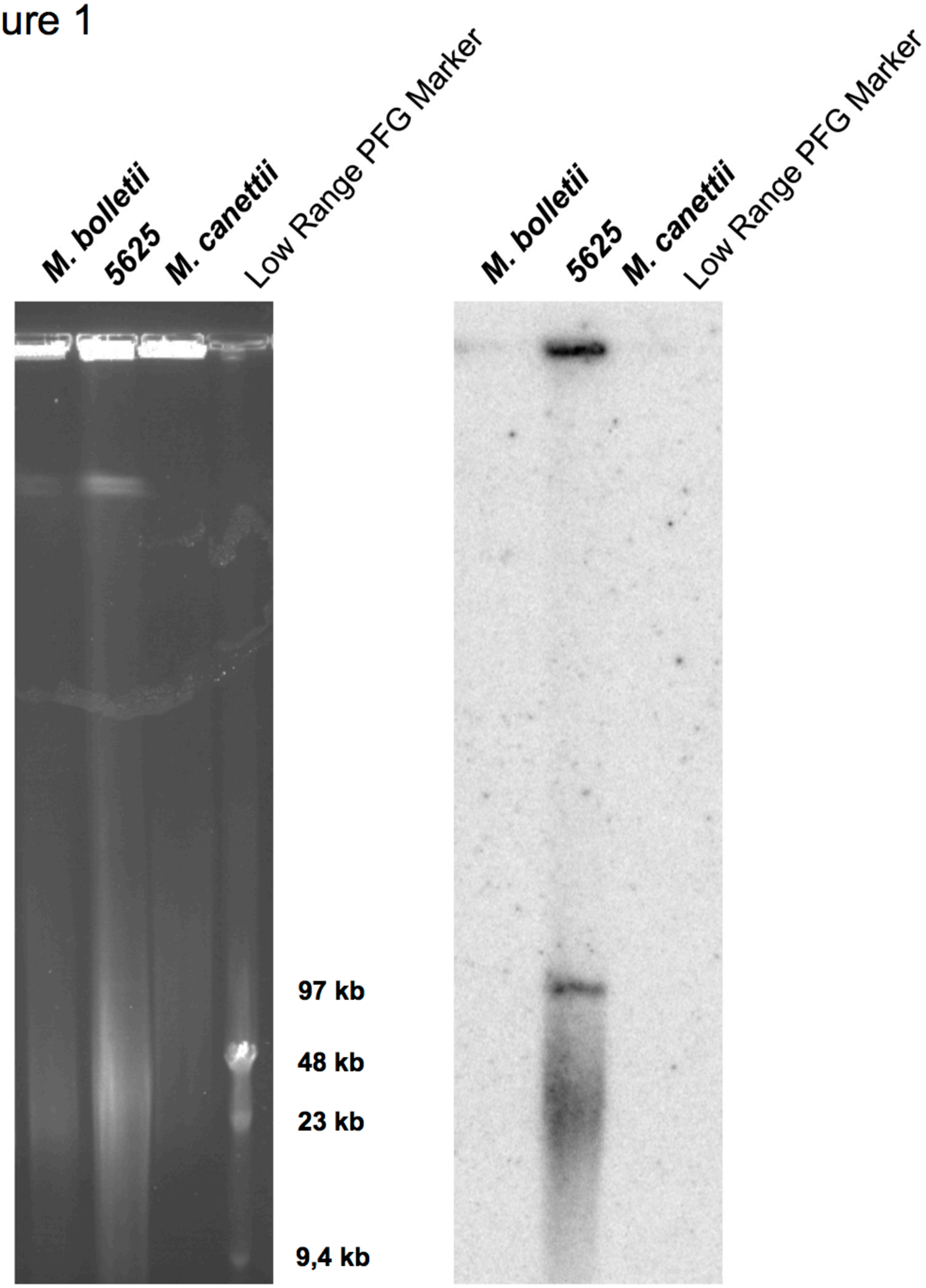
M. bolletii
5625
M. canettii
Low Range PFG Marker
97 kb
48 kb
23 kb
9,4 kb
M. bolletii
5625
M. canettii
Low Range PFG Marker

Figure 2A

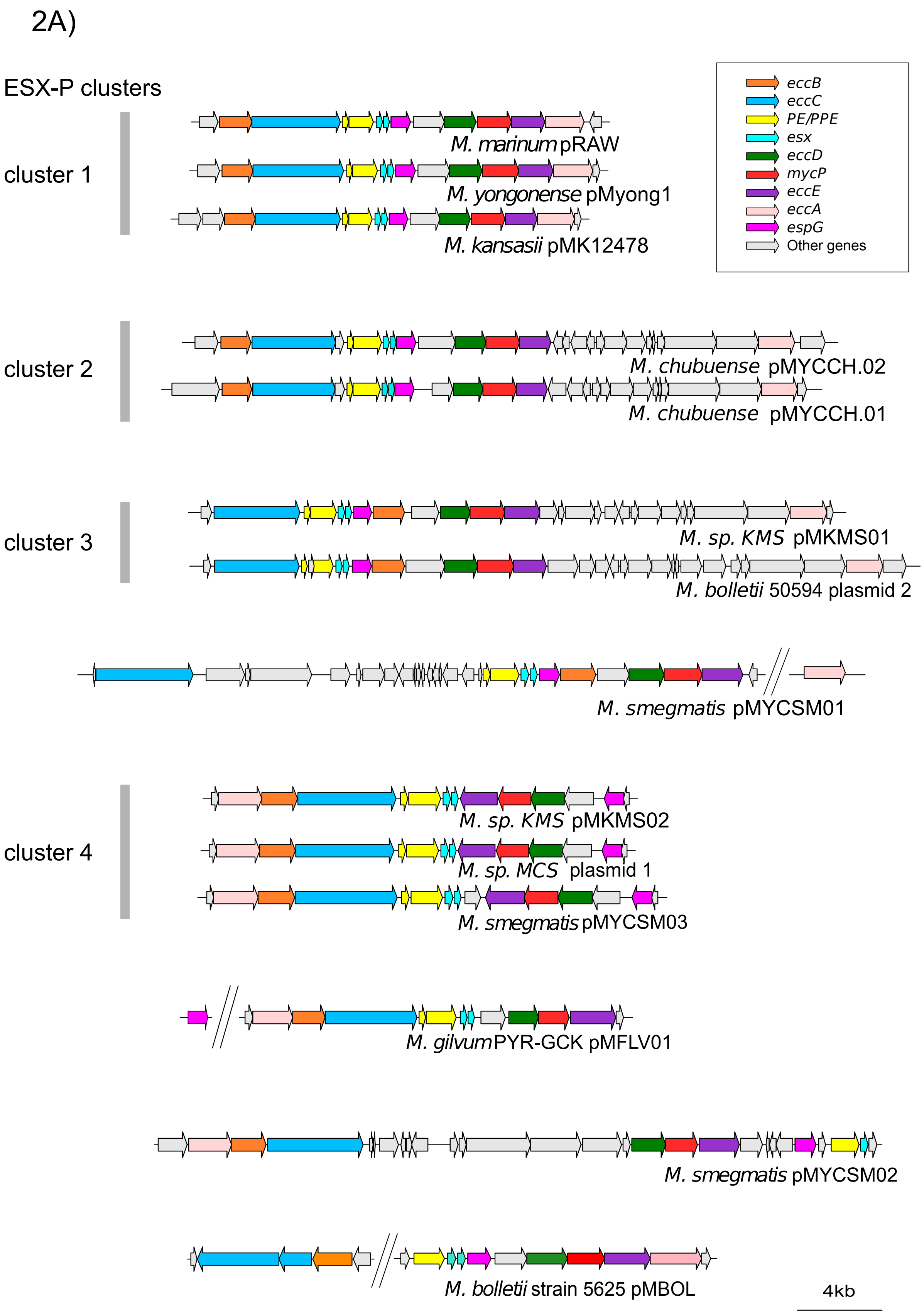
2A)
ESX-P clusters
cluster 1
M. marinum pRAW
M. yongonense pMyong1
M. kansasii pMK12478
eccB
eccC
PE/PPE
esx
eccD
mycP
eccE
eccA
espG
Other genes
cluster 2
M. chubuense pMYCCH.02
M. chubuense pMYCCH.01
cluster 3
M. sp. KMS pMKMS01
M. bolletii 50594 plasmid 2
M. smegmatis pMYCSM01
cluster 4
M. sp. KMS pMKMS02
M. sp. MCS plasmid 1
M. smegmatis pMYCSM03
M. gilvum PYR-GCK pMFLV01
M. smegmatis pMYCSM02
M. bolletii strain 5625 pMBOL
4kb

Figure 2B

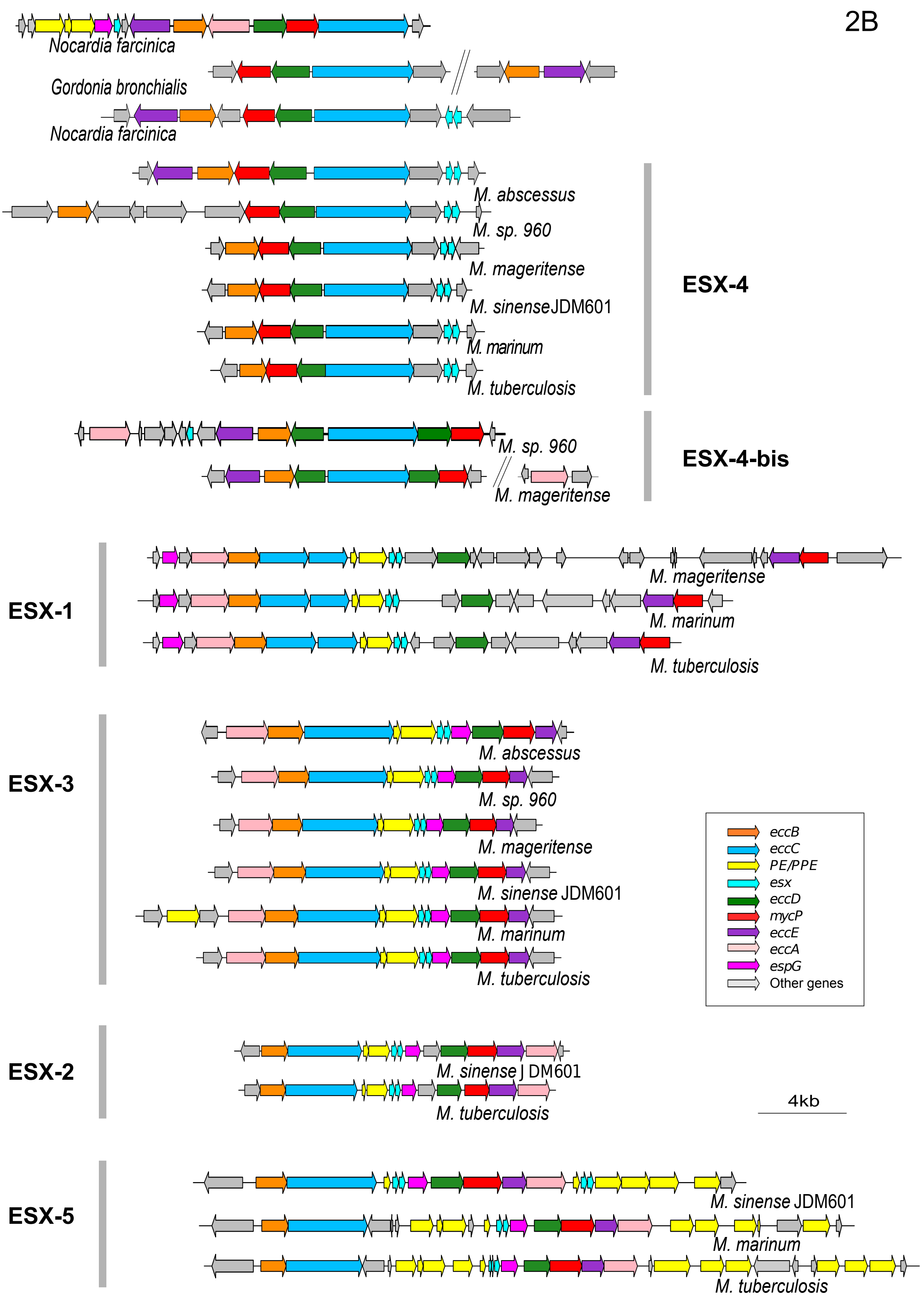
2B
Nocardia farcinica
Gordonia bronchialis
Nocardia farcinica
M. abscessus
M. sp. 960
M. mageritense
M. sinense JDM601
M. marinum
M. tuberculosis
ESX-4
M. sp. 960
M. mageritense
ESX-4-bis
ESX-1
M. mageritense
M. marinum
M. tuberculosis
ESX-3
M. abscessus
M. sp. 960
M. mageritense
M. sinense JDM601
M. marinum
M. tuberculosis
eccB
eccC
PE/PPE
esx
eccD
mycP
eccE
eccA
espG
Other genes
ESX-2
M. sinense J DM601
M. tuberculosis
4kb
ESX-5
M. sinense JDM601
M. marinum
M. tuberculosis

Figure 3

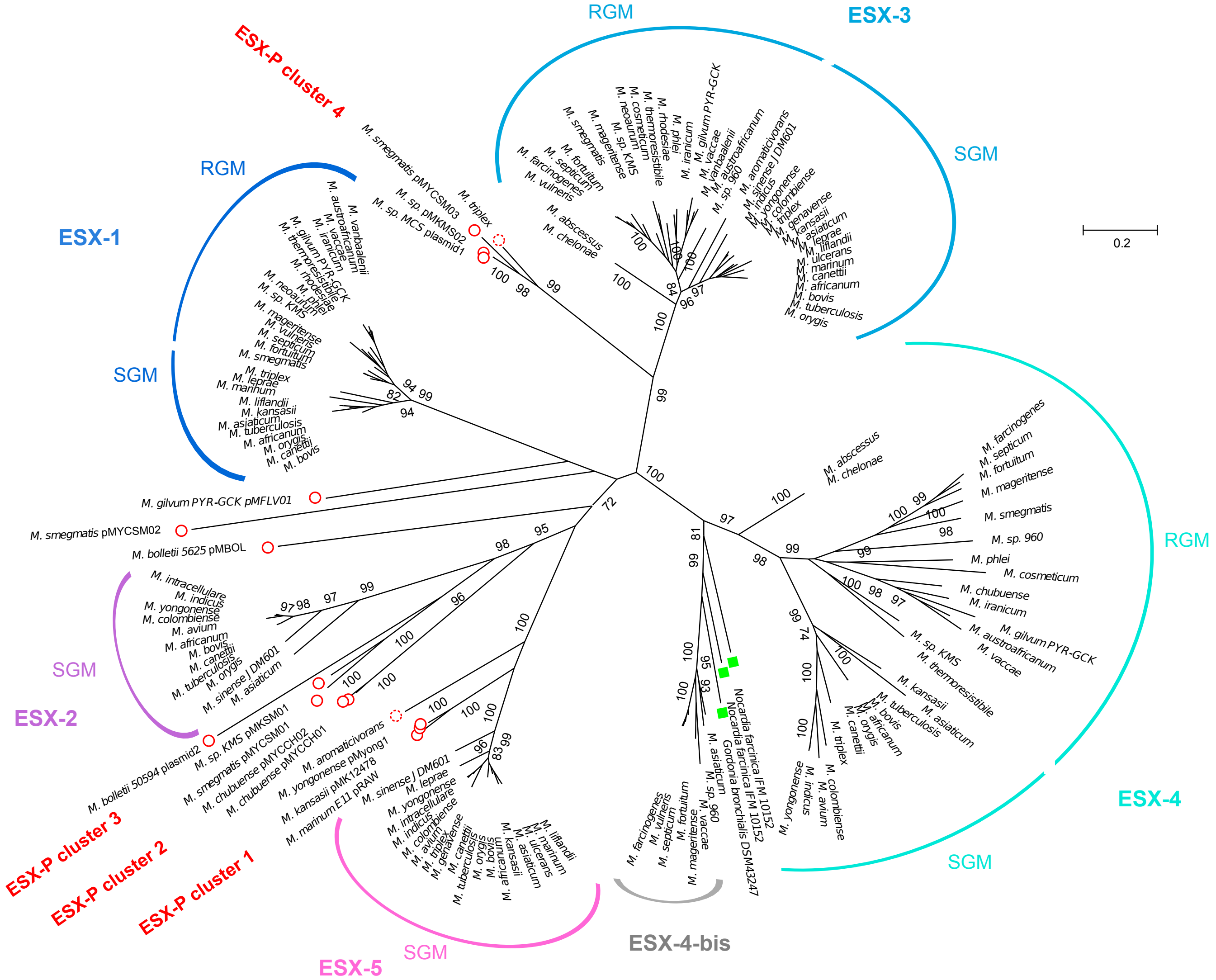
ESX-P cluster 4
RGM
ESX-3
SGM
RGM
ESX-1
SGM
RGM
ESX-4
SGM
ESX-4-bis
SGM
ESX-5
SGM
ESX-2
ESX-P cluster 3
ESX-P cluster 2
ESX-P cluster 1
0.2
M. smegmatis pMYCSM03
M. sp. pMKMS02
M. sp. MCS plasmid1
M. triplex
M. gilvum PYR-GCK pMFLV01
M. smegmatis pMYCSM02
M. bolletii 5625 pMBOL
M. bolletii 50594 plasmid2
M. sp. KMS pMKMS01
M. smegmatis pMYCSM01
M. chubuense pMYCCH02
M. chubuense pMYCCH01
M. aromaticivorans
M. yongonense pMyong1
M. kansasii pMK12478
M. marinum E11 pRAW
M. abscessus
M. chelonae
M. farcinogenes
M. septicum
M. fortuitum
M. mageritense
M. smegmatis
M. sp. 960
M. phlei
M. cosmeticum
M. chubuense
M. iranicum
M. gilvum PYR-GCK
M. austroafricanum
M. vaccae
M. sp. KMS
M. thermoresistibile
M. kansasii
M. asiaticum
M. tuberculosis
M. bovis
M. africanum
M. orygis
M. canettii
M. triplex
M. colombiense
M. avium
M. indicus
M. yongonense
Nocardia farcinica IFM 10152
Nocardia farcinica IFM 10152
Gordonia bronchialis DSM43247
M. asiaticum
M. sp. 960
M. vaccae
M. mageritense
M. fortuitum
M. septicum
M. vulneris
M. farcinogenes
M. liflandii
M. marinum
M. ulcerans
M. asiaticum
M. kansasii
M. africanum
M. bovis
M. orygis
M. tuberculosis
M. canettii
M. genavense
M. triplex
M. avium
M. colombiense
M. indicus
M. intracellulare
M. yongonense
M. leprae
M. sinense JDM601
M. intracellulare
M. indicus
M. yongonense
M. colombiense
M. avium
M. africanum
M. bovis
M. canettii
M. tuberculosis
M. orygis
M. sinense JDM601
M. asiaticum
M. vanbaalenii
M. austroafricanum
M. vaccae
M. iranicum
M. gilvum PYR-GCK
M. thermoresistibile
M. rhodesiae
M. neoaurum
M. phlei
M. sp. KMS
M. mageritense
M. vulneris
M. septicum
M. fortuitum
M. smegmatis
M. triplex
M. leprae
M. marinum
M. liflandii
M. kansasii
M. asiaticum
M. tuberculosis
M. africanum
M. orygis
M. canettii
M. bovis
M. vulneris
M. farcinogenes
M. septicum
M. fortuitum
M. smegmatis
M. mageritense
M. sp. KMS
M. neoaurum
M. cosmeticum
M. thermoresistibile
M. rhodesiae
M. phlei
M. iranicum
M. gilvum PYR-GCK
M. vaccae
M. vanbaalenii
M. austroafricanum
M. sp. 960
M. aromaticivorans
M. sinense JDM601
M. indicus
M. yongonense
M. colombiense
M. triplex
M. genavense
M. kansasii
M. asiaticum
M. leprae
M. liflandii
M. ulcerans
M. marinum
M. canettii
M. africanum
M. bovis
M. tuberculosis
M. orygis
M. abscessus
M. chelonae
100
98
99
100
99
100
72
95
98
97
99
97 98
96
100
100
100
100
100
100
96
83 99
100
84
96 97
100
99
94 99
82
94
100
97
100
99
100
100
98
99
98
99
100 98 97
99
74
100
100
100
81
99
100
95
93
100

Figure 4A

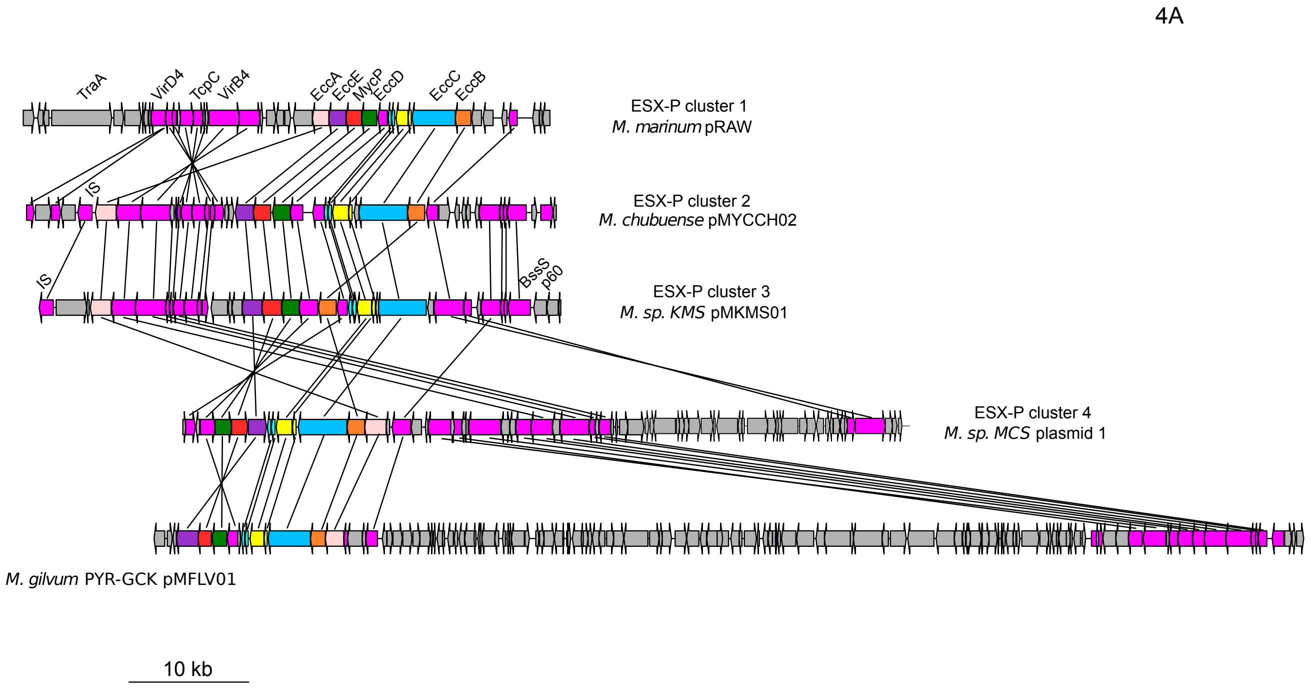
4A
TraA
VirD4
TcpC
VirB4
EccA
EccE
MycP
EccD
EccC
EccB
ESX-P cluster 1
M. marinum pRAW
IS
ESX-P cluster 2
M. chubuense pMYCCH02
IS
BssS
p60
ESX-P cluster 3
M. sp. KMS pMKMS01
ESX-P cluster 4
M. sp. MCS plasmid 1
M. gilvum PYR-GCK pMFLV01
10 kb

Figure 4B

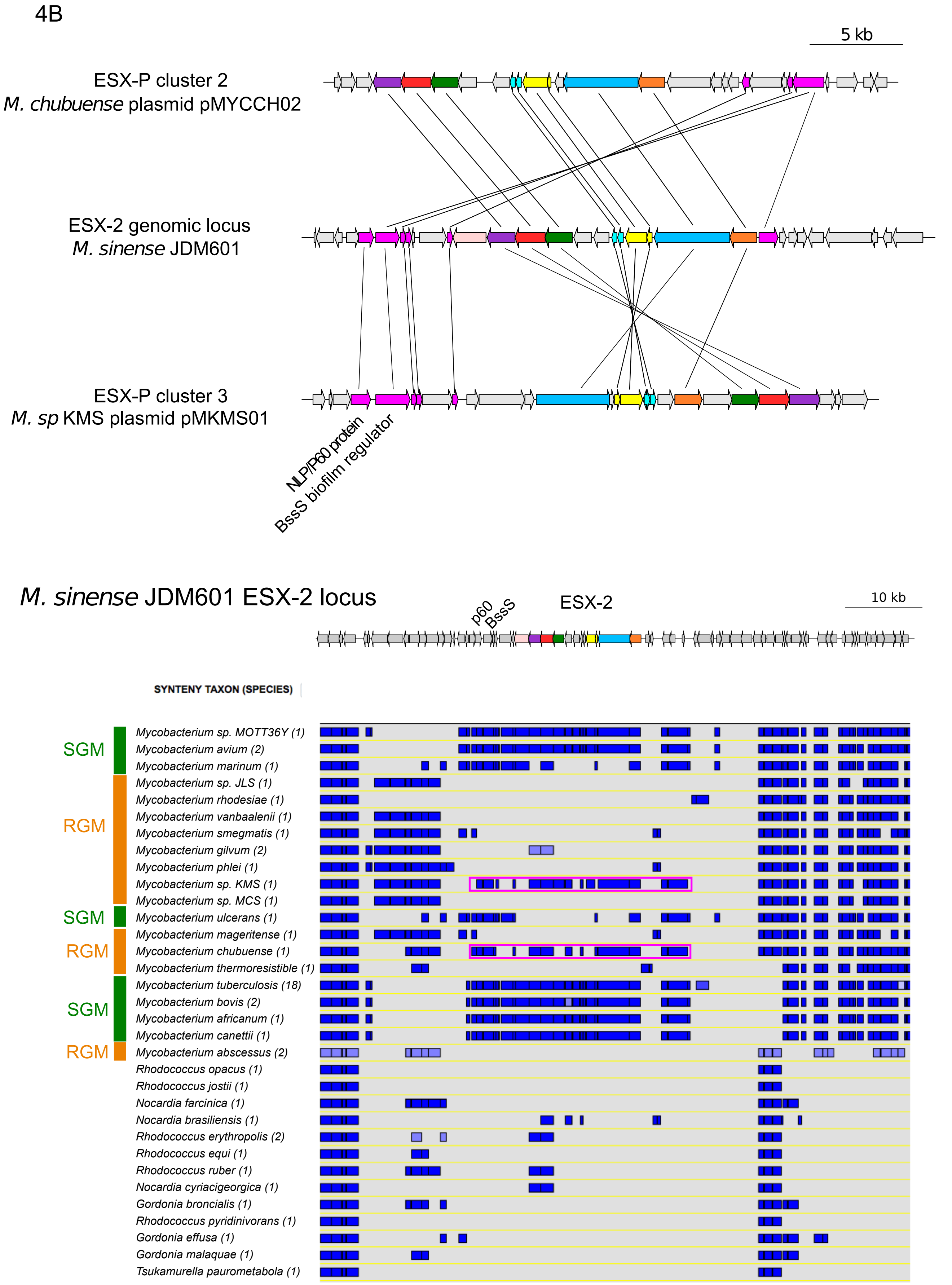
4B
5 kb
ESX-P cluster 2
M. chubuense plasmid pMYCCH02
ESX-2 genomic locus
M. sinense JDM601
ESX-P cluster 3
M. sp KMS plasmid pMKMS01
NLP/P60 protein
BssS biofilm regulator
M. sinense JDM601 ESX-2 locus
p60
BssS
ESX-2
10 kb
SYNTENY TAXON (SPECIES)
SGM
RGM
SGM
RGM
SGM
RGM
Mycobacterium sp. MOTT36Y (1)
Mycobacterium avium (2)
Mycobacterium marinum (1)
Mycobacterium sp. JLS (1)
Mycobacterium rhodesiae (1)
Mycobacterium vanbaalenii (1)
Mycobacterium smegmatis (1)
Mycobacterium gilvum (2)
Mycobacterium phlei (1)
Mycobacterium sp. KMS (1)
Mycobacterium sp. MCS (1)
Mycobacterium ulcerans (1)
Mycobacterium mageritense (1)
Mycobacterium chubuense (1)
Mycobacterium thermoresistible (1)
Mycobacterium tuberculosis (18)
Mycobacterium bovis (2)
Mycobacterium africanum (1)
Mycobacterium canettii (1)
Mycobacterium abscessus (2)
Rhodococcus opacus (1)
Rhodococcus jostii (1)
Nocardia farcinica (1)
Nocardia brasiliensis (1)
Rhodococcus erythropolis (2)
Rhodococcus equi (1)
Rhodococcus ruber (1)
Nocardia cyriacigeorgica (1)
Gordonia broncialis (1)
Rhodococcus pyridinivorans (1)
Gordonia effusa (1)
Gordonia malaquae (1)
Tsukamurella paurometabola (1)

Figure 5

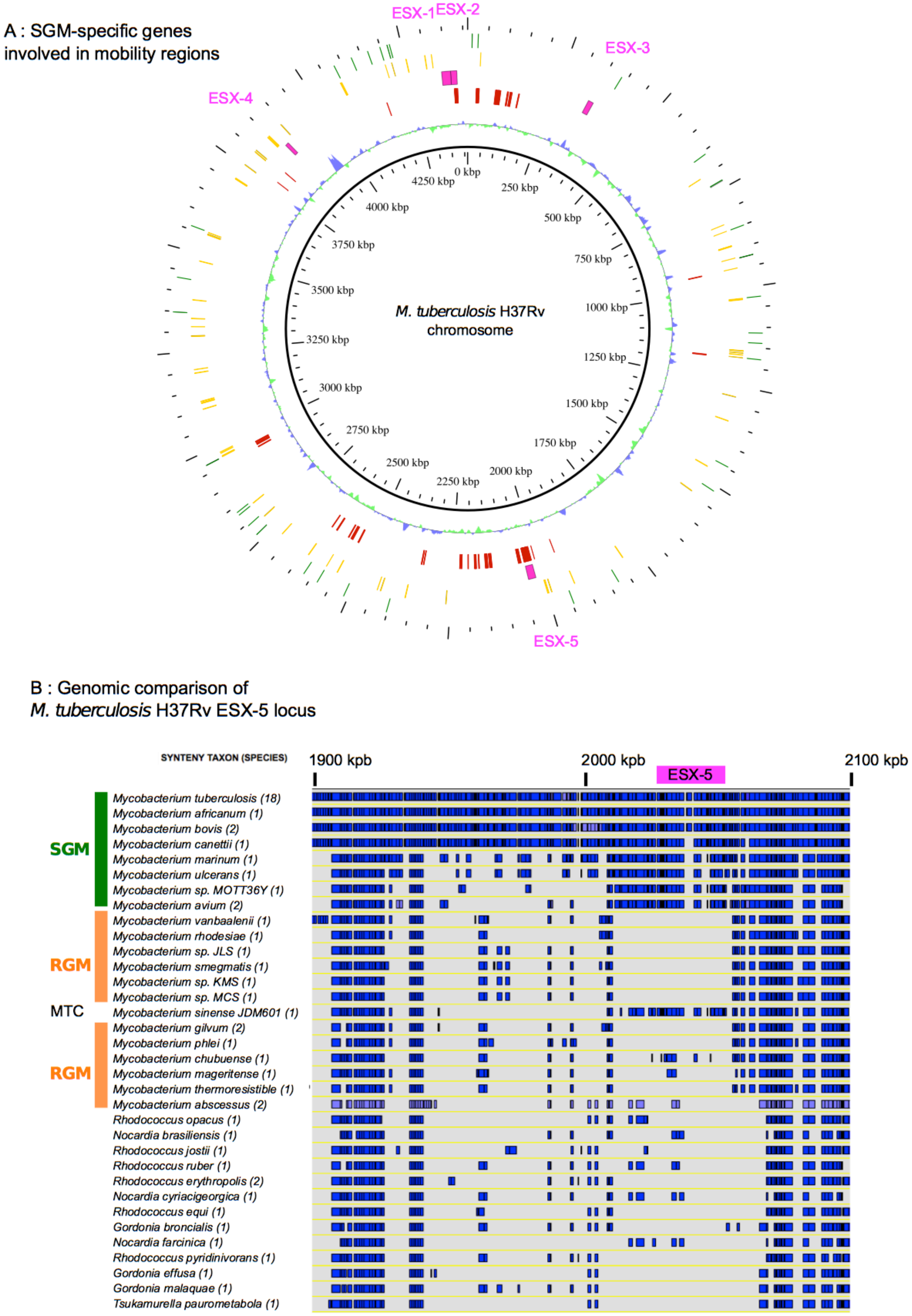
A : SGM-specific genes
involved in mobility regions
ESX-1
ESX-2
ESX-3
ESX-4
ESX-5
0 kbp
250 kbp
500 kbp
750 kbp
1000 kbp
1250 kbp
1500 kbp
1750 kbp
2000 kbp
2250 kbp
2500 kbp
2750 kbp
3000 kbp
3250 kbp
3500 kbp
3750 kbp
4000 kbp
4250 kbp
M. tuberculosis H37Rv
chromosome
B : Genomic comparison of
M. tuberculosis H37Rv ESX-5 locus
SYNTENY TAXON (SPECIES)
1900 kpb
2000 kpb
ESX-5
2100 kpb
SGM
RGM
MTC
RGM
Mycobacterium tuberculosis (18)
Mycobacterium africanum (1)
Mycobacterium bovis (2)
Mycobacterium canettii (1)
Mycobacterium marinum (1)
Mycobacterium ulcerans (1)
Mycobacterium sp. MOTT36Y (1)
Mycobacterium avium (2)
Mycobacterium vanbaalenii (1)
Mycobacterium rhodesiae (1)
Mycobacterium sp. JLS (1)
Mycobacterium smegmatis (1)
Mycobacterium sp. KMS (1)
Mycobacterium sp. MCS (1)
Mycobacterium sinense JDM601 (1)
Mycobacterium gilvum (2)
Mycobacterium phlei (1)
Mycobacterium chubuense (1)
Mycobacterium mageritense (1)
Mycobacterium thermoresistible (1)
Mycobacterium abscessus (2)
Rhodococcus opacus (1)
Nocardia brasiliensis (1)
Rhodococcus jostii (1)
Rhodococcus ruber (1)
Rhodococcus erythropolis (2)
Nocardia cyriacigeorgica (1)
Rhodococcus equi (1)
Gordonia bronchialis (1)
Nocardia farcinica (1)
Rhodococcus pyridinivorans (1)
Gordonia effusa (1)
Gordonia malaquae (1)
Tsukamurella paurometabola (1)